

# DESIGN OF A TRIPLE-BANDPASS FILTER USING A MODIFIED T-SHAPED RECTANGULAR COUPLED WITH A STEPPED IMPEDANCE RESONATOR FOR SMART PORTABLE COMMUNICATION DEVICE APPLICATIONS

## DIZAJN TRIPASOVNEGA FILTRA Z UPORABO MODIFICIRANEGA TRIPASOVNEGA PRAVOKOTIKA T-OBLIKE ZDRUŽENEGA S KORAČNIM IMPEDANČNIM REZONATORJEM V PAMETNIH PRENOSNIH NAPRAVAH ZA KOMUNIKACIJSKE APLIKACIJE

**M. Arulaalan<sup>1\*</sup>, Viswanathan Ramasamy<sup>2</sup>, R. Saravanakumar<sup>3</sup>, S. Maheswari<sup>4</sup>**

<sup>1</sup>Department of ECE, CK College of Engineering and Technology, Cuddalore, Tamil Nadu, India

<sup>2</sup>Department of CSE, Koneru Lakshmaiah Education Foundation, Vaddeswaram, AP, India

<sup>3</sup>Department of Wireless Communication, Institute of ECE, Saveetha School of Engineering, Savertha Institute of Medical and Technical Science, Chennai 602105, India

<sup>4</sup>Department of ECE, Panimalar Engineering College, Chennai, India

*Prejem rokopisa – received: 2023-04-03; sprejem za objavo – accepted for publication: 2023-05-11*

doi:10.17222/mit.2023.846

This paper presents a ground-breaking triple-bandpass filter design utilizing a modified T-shape rectangular coupled with a stepped impedance resonator (MTR-CSR) for smart portable communication device applications. The MTR-CSR filter operates at (2.2, 3.62 and 4.6) GHz, providing wide passbands in three operating modes. To achieve the optimal performance, the filter design is executed on a multi-layered liquid-crystal polymer (LCP) substrate with a thickness of 50  $\mu\text{m}$ , dielectric constant of 2.9 and loss tangent of 0.002. Simulation results for the MTR-CSR filter demonstrate a high level of accuracy and consistency with the measurement results for the fabricated filter. The filter exhibits an excellent stopband rejection, low loss and compact size while maintaining high-performance levels. Its performance parameters, such as insertion loss, return loss and group delay, are considered to evaluate the filter's performance. The results highlight the applicability of the MTR-CSR filter for smart portable communication devices.

**Keywords:** triple-bandpass filter, modified T-shape rectangular coupled with stepped impedance resonator, smart portable communication device applications, liquid-crystal polymer substrate, performance evaluation

V članku avtorji predstavljajo oblikovanje (dizajn) novega naprednega tripasovnega filtra z uporabo modificiranega pravokotnika T-oblike združenega s koračnim impedančnim rezonatorjem (MTR-CSR; angl.: Modified T-Shape Rectangular Coupled Stepped Impedance Resonator) v pametnih prenosnih napravah za komunikacijske aplikacije. MTR-CSR filter obratuje pri frekvencah 2,2 GHz, 3,62 GHz in 4,6 GHz in pri tem omogoča široko pasovno obratovanje na tri različne načine. Da bi dosegli optimalne lastnosti naprave so avtorji uporabili substrat (podlago) iz večplastnega polimera izdelanega na osnovi tekočih kristalov (LCP; angl.: liquid crystal polymer) debeline 50  $\mu\text{m}$ , z dielektrično konstanto 2,9 in tangensom izgub 0,002. Rezultati simulacij in meritev MTR-CSR filtra so pokazali njegovo veliko natančnost in konsistenco. Filter ponuja odlično zavrnitev (angl.: stopband rejection), majhne izgube in kompaktno velikost pri ohranitvi nivoja visoke kakovosti. Avtorji si izvedli evalvacijo njegovih performančnih parametrov kot so vztopne in povratne izgube ter zamuda skupine. Rezultati predstavljeni v pričujočem članku osvetljujejo uporabnost novega dizajna MTR-CSR filtra v pametnih napravah za komunikacijske aplikacije.

**Ključne besede:** tripasovni filter, modificiran pravokotnik T-oblike združen s koračnim impedančnim rezonatorjem, pametne prenosne komunikacijske naprave, substrat iz tekočega kristalnega polimera, ovrednotenje lastnosti.

## 1 INTRODUCTION

Today's demand for high-quality and reliable communication services has increased due to the extended wireless and ultra-wideband networks. A microwave filter is an essential component that operates the entire system and determines the range of frequency that can be allowed or restricted, depending on the application.<sup>1</sup> The next generation of 5G technology utilizes low-band, mid-band and millimeter wave band frequencies of

700 MHz, 3.5 GHz and 26 GHz. Bandpass filters are primarily used in these frequency ranges and they are designed to use resonators and various micro-elements that represent the properties of the filter. The miniaturization of bandpass filters is done to reduce parasitic elements with various planar miniaturization methods. Several research scholars have presented differently structured resonators, including the stepped impedance resonator, stub impedance resonator, stub-loaded stepped impedance resonator (SLSIR) and parallel-coupled microstrip lines.<sup>2</sup>

A tunable resonator filter has been designed for multi-wideband operations that operate at various modulation frequencies to meet the demands of various appli-

\*Corresponding author's e-mail:  
arulaalan@gmail.com

cations. Different filters have been designed to satisfy industrial demands for a triple passband. It is crucial that a passband can be adjusted to make the filter applicable to different requirements. A passband adjustment is made by adjusting the values to the expected values, but the bandwidth control may be challenging. In the case of a stepped impedance resonator (SIR), the frequency response is tuned by varying the stub, namely the open stub and short stub.<sup>3–5</sup> A filter is a device that processes frequency-dependent signals. The size of a filter depends on the resonators, which are the fundamental elements of the filter. Therefore, the resonator design used for a filter fabrication determines the size of the filter.<sup>6</sup> The filter size plays a significant role in many compact and advanced devices, especially in the case of compact wireless devices where a small and thin filter is required for integration. The miniaturization of filters is essential for reducing parasitic elements and improving the performance. Various planar miniaturization methods have been utilized to achieve this goal. These methods include using fractals, meander lines and interdigital structures.<sup>7–9</sup>

In recent years, there has been a growing demand for compact and cost-effective wireless devices that operate in multiple modes to meet various communication requirements. To achieve this, the size of microwave filters, essential components of the wireless communication system, must be reduced. This can be achieved by optimizing the size of the resonator that is the filter's basic element. Traditionally, the waveguide technology has been used to enhance the Q-value of the resonator. However, the bulky nature of waveguides limits their use in compact devices. Coaxial cavity resonators have been proposed as an alternative to waveguides for the compact-filter design to overcome this limitation.<sup>10,11</sup>

This study proposes a multi-mode resonator, a modified T-shaped rectangular coupled with a stepped impedance resonator (MTSR-CSIR), which operates at three resonant frequencies, by modifying the resonator structure. The width of the resonator is optimized to achieve the compact filter size. The MTSR-CSIR design exhibits significant advantages, including cost-effectiveness, simplicity of the structure, and high performance in different modes, making it a promising solution for future wireless communication devices.

The major contributions of the proposed MTSR-CSIR filter are as follows:

- **Tri-passband filter:** The modified T-shaped resonator is designed to pass the three bands at different resonant frequencies. The pass can be adjusted by varying the length of the resonator. As a result, the proposed filter covers frequency ranges of 2–2.5 GHz, 3.1–3.76 GHz, and 4.32–5.2 GHz, respectively.
- **Enhanced bandwidth:** The bandwidth of the passband is enhanced by varying the  $d_3$  width of the resonator. The isolation of three passbands is observed in the simulation results due to the adjustment of the resonator width. While improving the width of the reso-

erator, the bandwidth is enhanced. Thereby, the Q-factor of the filter will also be improved.

- **Rejection of undesired frequency:** The filter design has an additional rectangular resonator to eliminate the harmonic frequency beyond the passband frequency range. The rejection of undesired frequency enhances the performance of the TRCSIR filter.

The structure of this paper is as follows: Section 2 presents a review of previous work related to designing ultra-wideband filters for wireless applications operating in a multi-mode system. Section 3 presents the design of the proposed modified T-structured resonator with a rectangular coupled with a stepped impedance resonator. A resonator analysis is described in detail, followed by the MTSR-CSIR filter design. Simulation results for the proposed filter regarding the insertion and return loss are presented in Section 4. Finally, Section 5 concludes the paper by summarizing the MTSR-CSIR filter design and evaluating its performance.

## 2 RELATED WORKS

This literature survey explores the current research of the microwave filter design and its applications in wireless communication systems. We have discussed the importance of bandpass filters for meeting the demand for extended wireless and ultra-wideband networks. The use of tunable resonator filters for multi-band operations has been highlighted. We have seen how the filter size can be reduced by optimizing the resonator width and utilizing compact resonator structures.

In recent years, there has been a significant focus on designing and developing compact and efficient filters for wireless communication applications. Research studies have proposed various resonators and filter structures to achieve this goal. Dong-Sheng et al.<sup>12</sup> presented the design of a UWB bandpass filter that operates between 3.1 GHz and 10.6 GHz. The filter consists of a WLAN notch combined with a BPF at 5.8 GHz and a microstrip structure, which provides a 108 % bandwidth. The filter achieved a return loss of approximately 1.0 dB at 6.85 GHz, indicating that it can effectively pass the broad passband frequency while rejecting the high stopband suppression. The filter is suitable for integration into small devices and antennas due to its compact size.

Wang et al.<sup>13</sup> proposed a small bandpass Wilkinson power divider with UWB harmonic reduction. The proposed model suppresses the DC component and third-, fifth- and seventh-order harmonic components. The frequency-selecting coupling structure unit is the central component for harmonic suppression. The dimensions of the WPD are 14.65 mm × 19.64 mm, and it has a return loss above -3.4 dB at the operating frequency, with a bandwidth of -20 dB, or 1.74 GHz to 3.71 GHz. The tuning of the WPD was accomplished by modifying the resonators' length and breadth. The bandpass WPD com-

pletely rejects the harmonic components. This design is an efficient solution for UWB systems, requiring a small size and high performance.

Zheng et. al.<sup>14</sup> proposed a defected structure of a microstrip to create a bandpass filter with incorporated switches in the defected T-shaped structure to adjust the frequency. The filter has a dual-band gap and is suitable for a cognitive radio with minimal distortion. Passband frequencies were achieved using a 0.25 mm wide hole and gap. A wideband antenna with dimensions of 65 mm by 40 mm was designed, and a switch was incorporated to change the slot height, thereby tuning the frequency as required.

Al-Shalaby et al.<sup>15</sup> designed a novel band-stop filter by utilizing a defected ground structure in the form of a dumbbell and a U-shaped cavity on microstrip lines. The proposed filter achieved a remarkable notch depth of -39.13 dB for the 1.4 GHz resonant frequency, surpassing the performance of conventional dumbbell filters with a notch depth of -32.21 dB for the 2.6 GHz resonant frequency. The spiral dumbbell shape contributed to a high Q-value of 8.823, demonstrating the proposed design's effectiveness in suppressing unwanted frequencies.

Tantivivat et al.<sup>16</sup> proposed the multi-mode SLR to design a compact tri-band BPF, but it suffered from a narrow frequency range and high insertion loss. To address these issues, the interaction between two multi-mode resonators, such as stepped-impedance resonators (SIRs) in tri-band and dual-band BPFs and SLRs in tri-band and dual-band BPFs, was utilized to achieve passband contributions from both odd and even bands. Ren et.al.<sup>17</sup> proposed a modified approach where two SIRs were coupled to create a compact dual-band bandpass filter. However, this resulted in a significant insertion loss and narrow passbands. Another approach involved dividing a passband into multiple passbands and adding structures with stopbands or transmission zeros (TZs) to BPFs or low-pass filters.

Wang et al.<sup>18,19</sup> presented a novel dual-band graphene microstrip filter for 5G applications, but its adoption is limited due to a high insertion loss. However, there is a

lack of research on tri-band BPFs that can meet the requirements for small-size, low-loss and wide passbands for 5G mobile communication systems. The above highlights the need for further investigation and development of tri-band BPFs that can effectively address the challenges of 5G communication systems.

Hou et al.<sup>20</sup> proposed the development of a dual-wideband and a tri-wideband BPF for 5G mobile communications. The dual-wideband BPF is created using two folded open-loop stepped-impedance resonators (FOLSIRs). In comparison, the tri-wideband BPF is achieved by inserting two folded uniform impedance resonators (FUIRs) into the dual-wideband BPF. A unique structural deformation of SIR produces a FOLSIR in the filters. However, the proposed filters may still have physical-dimension and insertion-loss limitations. In response to this review, we propose a three-passband filter utilizing the modified T-structured resonator and a rectangular slot-coupled filter to reject undesired frequencies.

### 3 EXPERIMENTAL PART

#### 3.1 Analysis of the modified T-resonator

The MTSR-CSIR filter incorporates the modified T-resonator in its design, which is analyzed as follows. The modified T-resonator comprises a low- and a high-impedance section, both on either side of a  $\lambda/2$  SIR. The length of the low-impedance section is  $\lambda/4$ , while the length of the high-impedance section is  $\lambda/8$ . **Figure 1** shows the equivalent circuit of the resonator's impedance circuit. The resonator's characteristic impedance and electrical length are denoted by  $Z_1$  and  $Z_2$ , respectively. The electrical length of the low-impedance and high-impedance sections are represented by  $\deg 2\theta$  and  $\theta$ , respectively. The following expressions relate to the resonant frequency, characteristic impedance and electrical length:

$$\theta_i = \arctan \sqrt{X_Z} \tag{1}$$

$$\frac{f_{d7}}{f_0} = \frac{\pi/2}{\arctan \sqrt{X'_Z}} \tag{2}$$

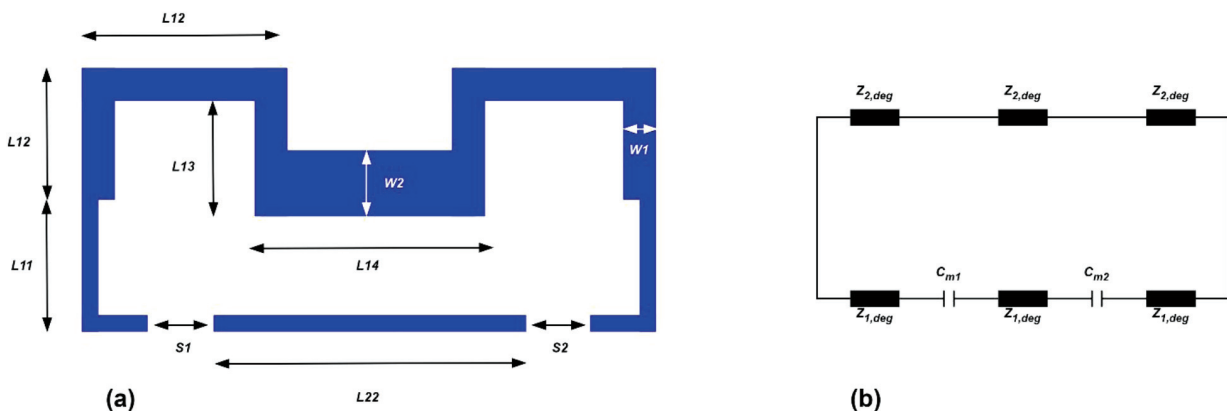


Figure 1: Equivalent impedance diagram for the modified T-SIR

Here,  $f_0$  denotes the resonant frequency of the modified T-SIR,  $\theta_i$  is the instant electrical length of the resonator, and  $i$  is the ratio of low and high characteristic impedance parts. The characteristic impedance of an individual region is given by

$$Z_0 = \frac{\pi}{\sqrt{\epsilon}} \cdot \frac{1}{\frac{w_r}{120} + 1.393 + 0.667 \ln\left(\frac{w_r}{h} + 1.44\right)^r} \quad (3)$$

$$\epsilon = \frac{\epsilon_{r+1}}{2} \left( 1 + \left( 1 + \frac{12h_r}{w_r} \right)^{\frac{1}{2}} \right) \quad (4)$$

The physical dimensions of the modified T-resonator are analyzed with respect to Equations 1 and 4, considering the substrate material of the filter with the width  $w_r$ , thickness of the ground plane  $h_r$  and dielectric constant  $\epsilon_r$ . The resonant and second harmonic frequencies  $f_{d7}$  are calculated based on these parameters. The modified T-SIR's physical length is reduced to improve the transmission zeros in the passband. The difference in the transmission line impedance is balanced by varying  $d_3$ . The simulation response of S21 for varying lengths of the resonators is analyzed and presented in **Figure 2**.

The input impedance of the individual impedance part is expressed as

$$|Z_{in}(d)| = \left| Z_0 \frac{z_x + jz_0 \tan \alpha x}{z_0 + jz_x \tan \alpha x} \right| \quad (5)$$

$$|Z_{in}| = \left| Z_0 \frac{z_x + jz_0}{z_0 + jz_x} \right| \quad (6)$$

The resonant frequency of the modified T-resonator is determined with Equation (6) where  $Z_0$  represents the characteristic impedance,  $Z_x$  represents the load impedance, and  $\text{deg}$  is denoted as  $\alpha x$ . The parameters of the substrate and resonator, such as the electrical length, fre-

quency and length, are obtained with the following expressions after determining the substrate parameters:

$$q_i = \infty x \quad (7)$$

$$\infty = \frac{\pi}{\gamma'_g / 2} \quad (8)$$

$$\gamma'_g = \frac{\gamma_0}{\sqrt{\epsilon_g}} \quad (9)$$

Theoretical analysis of the proposed filter is based on Equations (4), (7) and (9). The effect of varying distance  $d_7$  on the filter performance is studied by changing its value from 3.5 mm to 5.5 mm. The simulation results of the filter response for different values of  $d_7$  are shown in **Figure 2a**, and the filter's frequency response is shown in **Figure 2b** based on the simulation analysis.

To meet the requirements of industrial applications, the physical dimensions of the filter are adjusted. To improve the S21 response, the  $d_7$  length is varied from 5.5 mm to 3.5 mm. The S21 response is enhanced by increasing the length of the resonator. The frequency suppression after 4.8 GHz is demonstrated for  $d_7 = 5.2$  mm and 5.5 mm. The length of 5.5 mm is found to achieve the desired cutoff frequency of the passband region.

### 3.2 Design of the triple-bandpass filter

In the previous section, we discussed the theoretical analysis of the resonator needed for designing a triple-bandpass filter. Now, we present the physical dimensions of the proposed MTSR-CSIR filter, as shown in **Figure 3**. The input is fed through a 50-ohm transmission line, and the coupling distance is reduced to enhance the quality factor of the filter. We analyze the response of the proposed filter using an EM simulator and evaluate the insertion loss and return loss through simulations. We vary the length of  $d_3$  to improve the passband width.

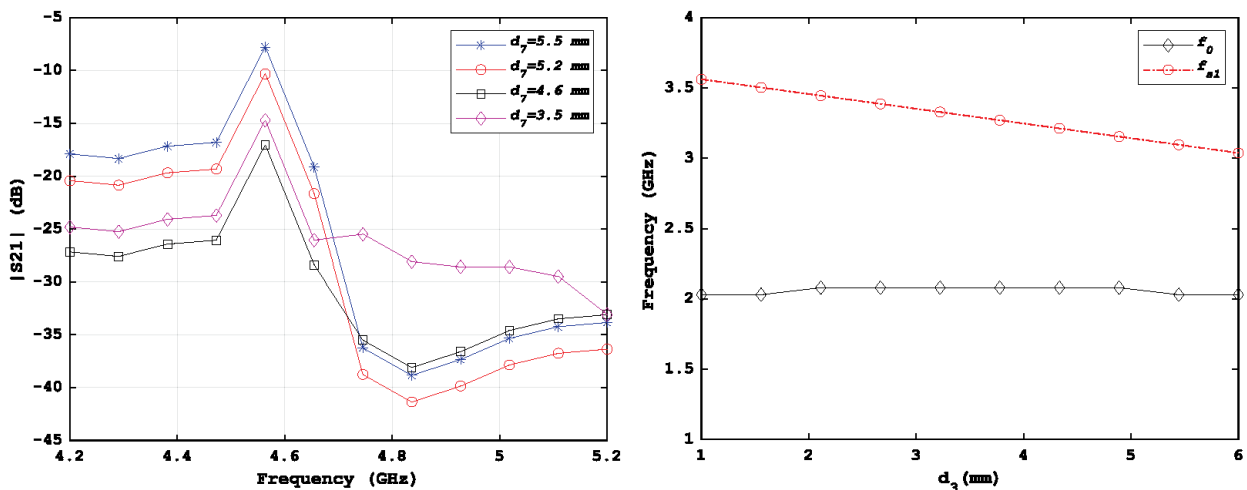
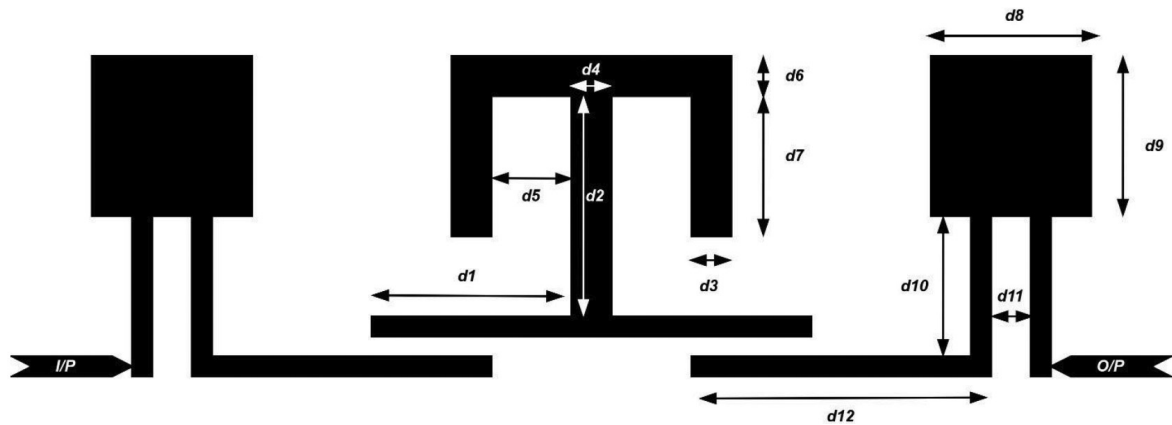


Figure 2: Simulation result of S21: a) analysis of various  $d_3$  lengths, b) response of resonant frequency  $f_0$  and  $f_{d7}$



**Figure 3:** Design of modified T-shaped rectangular coupled with triple-bandpass filter. The dimensions:  $d1 = 6$  mm,  $d2 = 7$  mm,  $d3 = 0.6$  mm,  $d4 = 2$  mm,  $d5 = 0.5$  mm,  $d6 = 1$  mm,  $d7 = 5.5$  mm,  $d8 = 2.1$  mm,  $d9 = 6.5$  mm,  $d10 = 2.2$  mm,  $d11 = 0.2$  mm,  $d12 = 5.5$  mm

The transmission zeros in the passband of the TRCSIR filter help suppress the resonant frequency and improve the passband bandwidth. The physical length of the coupling section,  $d2$ , is responsible for turning the passband frequency. During the design process, the widths of  $d3$  and  $d7$  are varied to obtain the desired results for the frequency range of 1–5 GHz, as shown in **Figure 3**. Furthermore, the spacing between the bent T-structure,  $d5$ , is reduced and adjusted to achieve the desired response. The coupling effect between the microstrip lines of the MTSR-CSIR filter enhances the overall quality factor of the triple-bandpass filter.

The width of the  $d3$  resonator is a significant factor affecting the filter's passband. The modified T-resonator in the middle section of the proposed design enables the filter to achieve triple passbands that cover the frequency range of 1–5 GHz. A rectangular slot is added to the modified T-structure to reject undesired frequencies beyond the 5 GHz frequency range. The transmission zeros of the passbands are improved by varying the  $d3$  width of the MTSR-CSIR filter. To achieve the desired frequency range, the  $d3$  dimension is reduced from 1 mm to 0.6 mm. The variation in the  $d3$  width and its impact on the passband response is shown with the simulation results presented in **Figure 4**.

The  $d12$  length is varied to achieve the desired tuning of the three-pass band in the designed filter. The  $d7$  width is also adjusted to place the resonant frequency of the three passbands to the desired frequency range. The  $d3$  dimension is optimized to enhance the transmission zeros of the passband. The simulation analysis of  $S_{21}$ , adjusting  $d7$  was discussed in the previous section. Once the physical dimensions of the filter are optimized, the designed filter is fabricated on a multi-layered LCP substrate with a thickness of 50  $\mu\text{m}$ , a dielectric constant of 2.9 and a loss tangent of 0.002. The filter's performance is evaluated using the EM simulation results, including the insertion loss, return loss and group delay. The resulting filter covers the frequency range of 1–5 GHz, with three passbands at (2.2, 3.62 and 4.6) GHz, respectively, and exhibits excellent performance.

## 4 RESULTS AND DISCUSSION

A novel triple-bandpass filter is proposed in this work, utilizing a modified T-shaped resonator to design an MTSR-CSIR filter. The physical dimensions of the filter are carefully adjusted to achieve the desired frequency range. The bent/modified T-structure is the main component of the MTSR-CSIR filter, which enables the filter to have the desired passband frequency response. The resonant frequency response is derived theoretically, and the simulation results are presented in **Figure 2b** and discussed in Section 3. Additionally, a rectangular coupled with a resonator is incorporated to improve the filter's performance further. The undesired frequency is suppressed by adjusting the  $d7$  dimension of the filter.

The three-pass band is adjusted by varying the  $d12$  length, while the transmission zeros of the passband are improved by adjusting the  $d3$  dimension. The  $d7$  width is also varied and analyzed to place the resonant frequency of the three passbands within the desired frequency range. The simulation analysis of  $S_{21}$  for adjusting  $d7$  is shown in **Figure 2a** and discussed in Section 3. After the optimization of the physical dimensions of the filter, the designed filter with unique physical dimensions is fabricated on a multi-layered LCP substrate with a thickness of 50  $\mu\text{m}$ , dielectric constant of 2.9 and loss tangent of 0.002. The EM simulation results, including performance parameters, such as the insertion loss, return loss and group delay, are considered to evaluate the performance of the MTSR-CSIR filter.

The EM simulation results are used to evaluate the performance of the MTSR-CSIR filter, considering the performance parameters, such as the insertion loss, return loss and group delay. The resultant filter covers a frequency range of 1–5 GHz, with three passbands at 2.2, 3.62 and 4.6 GHz, respectively. The simulated response effectively suppresses the transmission zeros at each passband frequency range.

In this proposal, the  $d3$  width of the modified T-shaped resonator is varied to enhance the passband response of the triple-bandpass filter. The  $d3$  width is a

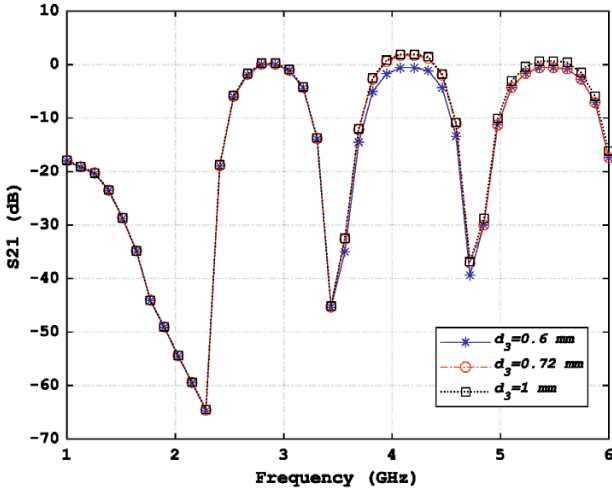


Figure 4: S21 response analysis for different dimensions of  $d_3$

critical parameter that influences the bandwidth of the passband response. The effect of varying the  $d_3$  value on the passband response is analyzed through the simulation.

The simulation results, as shown in **Figure 4**, indicate that increasing the  $d_3$  value improves the passband response. If the width is too narrow, like 0.6 mm, the passband response is very narrow, which is unsuitable for practical applications. In contrast, if the width is increased to 1 mm, the bandwidth of the passband response is enhanced significantly, which is desirable for practical applications.

Therefore, the  $d_3$  width is set to 1 mm to achieve the desired passband response. This enables the passband to shift to the expected frequency region while increasing the bandwidth of the passband response. Overall, varying the  $d_3$  value significantly impacts the passband response of the triple-bandpass filter, and proper optimization of this parameter is crucial for achieving the optimal filter performance.

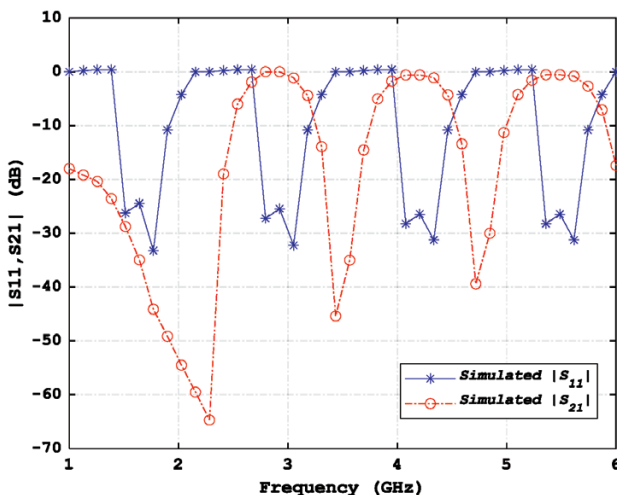


Figure 5: Comparative analysis of simulated S11 and S21 response of the proposed MTSR-CSIR filter

The EM simulator simulates the entire filter design after optimizing all the physical dimensions. **Figure 5** displays the simulation results for the return loss S11 and insertion loss S21 parameters for the proposed modified MTSR-CSIR filter design.

The simulation results of the MTSR-CSIR filter design indicate that it achieved high performance in terms of both return loss and insertion loss. The  $|S_{11}|$  filter response demonstrates a high return loss, with values of -65 dB at 2.2 GHz, -46 dB at 3.62 GHz and -40 dB at 4.6 GHz for the three passbands of the filter. This implies that the filter has a very low reflection loss, which means that most of the input signal is transmitted to the output port with a minimal power loss.

Furthermore, the simulation response of the  $|S_{21}|$  parameter shows that the designed filter achieves a low insertion loss at the cutoff frequencies. It achieves low insertion losses of 0.62 dB at 2.2 GHz, 0.65 dB at 3.62 GHz, and -0.71 dB at 4.6 GHz for the three passbands of the filter. This indicates that the filter effectively passes signals in the desired frequency range while suppressing the signals in the unwanted frequency range.

The MTSR-CSIR filter operates at three simultaneous passbands covering the frequency range of 2–2.5 GHz, 3.1–3.76 GHz and 4.32–5.2 GHz. The bandwidth of the passbands is also wide enough to allow the passage of the required signals.

The designed triple-passband filter exhibits effective signal-selection performance for the propagated signal, as demonstrated by the simulation of the electric-field distribution. The filter was fabricated and analyzed using a network analyzer, and it was applied to wireless communications. The simulated results closely match the measured results, as seen in **Figure 6**. The fractional bandwidth (3 dB) at the passband frequencies of (2.2, 3.62 and 4.6) GHz is (16, 14.3 and 11.52) %, respectively. The high return loss and low insertion loss achieved by the designed filter make it an efficient signal selector in the frequency range of 2–5 GHz.

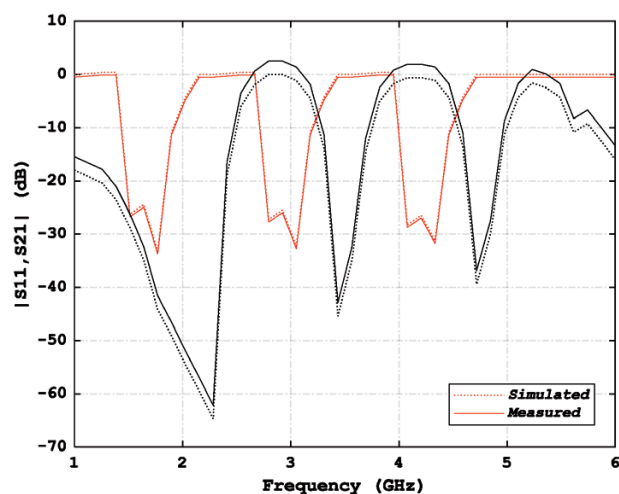
The filter suits various wireless communication applications like WLAN, Bluetooth and WiMax. The filter’s ability to simultaneously pass three different frequency bands allows it to be used in multi-band wireless communication systems. The fabricated filter also demonstrates good stability, making it a suitable choice for harsh environments. The proposed MTSR-CSIR filter design is an effective and efficient solution for wireless communication systems requiring a triple-passband filter with high-performance parameters.

The transmission zeros of the three passbands are observed at (1.5, 2.72 and 4.6) GHz, and the filter can effectively isolate the three passbands. The rectangular slot eliminates the undesired frequencies after 5.2 GHz.

A comparative analysis of different triple-bandpass filters includes the following data: center frequencies abbreviated as CF (GHz), defected ground structure abbreviated as DGS, fractional bandwidth abbreviated as

**Table 1:** Comparison of the proposed MTSR-CSIR filter with other triple-passband filters

Tri-band filter	DGS	CF	FBW	IL	RL
FUIR	No	2.17/3.51/4.86	12.4/11.4/13.3	0.46/0.49/1.3	32/33/11.6
MTM	Yes	2.41/3.56/5.29	6.2/12.2/11.8	1.9/1.421/5.1	14.3/15/16.8
MW-BPF	Yes	2.45/3.5/5.2	9.6/13.1/7.9	1.2/1.5/1.6	16.3/17.9/12.9
Coupling MBF	No	2.5/3.6/5.1	4.0/4.0/6.0	2.9/2.7/2.3	>17
UIR	Yes	1.8/3.5/5.8	8.9/12.5/5.3	1.5/0.9/2.9	15/23/11.6
MTSR-CSIR (Proposed)	No	2.2/3.62/4.6	16/14.3/11.52	0.62/0.65/0.71	65/46/40

**Figure 6:** Comparison of the measured and simulated frequency response of the MTSR-CSIR filter

FBW (%), insertion loss abbreviated as IL in (dB), and return loss abbreviated as RL in (dB).

**Table 1** presents a comparative analysis of the proposed MTSR-CSIR filter and various other triple-passband filters reported in the literature. The results show that the proposed filter performs better than the FUIR, MTM, MW-BPF, coupling MBF and UIR filters. The MTSR-CSIR filter achieves an enhanced bandwidth and low insertion loss with a compact physical size.

The MTSR-CSIR filter has a simple structure with a low fabrication complexity, making it a cost-effective and practical solution for various wireless communication applications. Center frequencies of 2.2/3.62/4.6 GHz relating to the three passbands are achieved by the MTSR-CSIR filter. Furthermore, fractional bandwidths of about 16/14.3/11.52 %, respectively, are achieved with the MTSR-CSIR filter, which is higher than with the other filters.

The insertion loss obtained by the MTSR-CSIR filter is 0.62/0.65/0.71, respectively, lower than that of the other filters. The return loss of the proposed filter is also superior, achieving values of 65/46/40, respectively. A defected ground-structure filter is also considered in the comparison, and the MTSR-CSIR filter outperforms it in terms of its simple structure and superior performance.

The comparative analysis shows that the proposed MTSR-CSIR filter performs better than the other filters. The filter has a compact physical size, low insertion and high return loss, making it an ideal candidate for wireless

communication applications. The simple structure of the MTSR-CSIR filter also makes it easy to fabricate and implement.

## 5 CONCLUSION

The proposed MTSR-CSIR filter is compact and simple, without any defected structure in the ground plane. The modified T-shaped resonator includes a highly applicable triple-bandpass filter. The physical dimensions of the filter are adjusted to tune the desired frequency. The proposed MTSR-CSIR filter is compared with the existing tri-BPFs, such as the FUIR filter, MTM filter, MW-BPF filter, coupling MBF filter and UIR filter. The simulation results show the center frequencies of 2.2/3.62/4.6 GHz for the three passes. The fractional bandwidth achieved by the MTSR-CSIR is about 16/14.3/11.52 %, respectively. The insertion loss obtained by the filter is 0.62/0.65/0.71, respectively, and the return loss of the proposed BPF is about 65/46/40, respectively. The triple-passband BPF exhibited an effective signal-selection performance for the propagated signal, as demonstrated by the simulation of the electric-field distribution. The results show that the proposed MTSR-CSIR applies to 5G mobile communications. The proposed MTSR-CSIR filter outperforms the existing tri-BPFs regarding bandwidth, insertion loss and physical size. The MTSR-CSIR filter has a simple structure with low fabrication complexity, making it a cost-effective solution for 5G communication systems. The proposed MTSR-CSIR filter is a compact, simple, cost-effective solution for tri-band filtering applications. The filter achieves the desired center frequency and fractional bandwidth with a low insertion loss and high return loss. The filter's simple structure and improved performance make it an excellent candidate for 5G mobile communication systems.

## Declaration of competing interest

The authors declare that there are no known competing financial interests or personal relationships that could have influenced the work reported in this paper.

## 6 REFERENCES

- <sup>1</sup> M.-H. Weng, S.-W. Lan, S.-J. Chang, R.-Y. Yang, Design of Dual-Band Bandpass Filter with Simultaneous Narrow- and Wide-Bandwidth and a Wide Stopband, *IEEE Access*, 7 (2019), 147694–147703, doi:10.1109/ACCESS.2019.2946302

- <sup>2</sup> A. Lalbakhsh, S. M. Alizadeh, A. Ghaderi, A. Golestanifar, B. Mohamadzade, M. Jamshidi, K. Mandal, W. A. Mohyuddin, Design of a Dual-Band Bandpass Filter Based on Modal Analysis for Modern Communication Systems, *Electronics*, 9 (2020), 1770, doi:10.3390/electronics9111770
- <sup>3</sup> T.-H. Lee, K.-C. Yoon, K. G. Kim, Miniaturized Dual-Band Bandpass Filter Using T-Shaped Line Based on Stepped Impedance Resonator with Meander Line and Folded Structure, *Electronics*, 11 (2022), 219, doi:10.3390/electronics11020219
- <sup>4</sup> S. Dey, S. K. Koul, Reliable, Compact, and Tunable MEMS Bandpass Filter Using Arrays of Series and Shunt Bridges for 28-GHz 5G Applications, *IEEE Transactions on Microwave Theory and Techniques*, 69 (2021), 75–88, doi: 10.1109/TMTT.2020.3034182
- <sup>5</sup> X. Zhu, Z. Ge, L. Yang, R. Gómez-García, Millimeter-Wave CMOS Passive Filters for 5G Applications, 2021 IEEE MTT-S International Microwave Filter Workshop (IMFW), Perugia, Italy, 2021, 198–200, doi:10.1109/IMFW49589.2021.9642358
- <sup>6</sup> S. Palanisamy, B. Thangaraju, O. I. Khalaf, Y. Alotaibi, S. Alghamdi, Design and synthesis of multi-mode bandpass filter for wireless applications, *Electronics*, 10 (2021), 2853, doi:10.3390/electronics10222853
- <sup>7</sup> H. Campanella, Y. Qian, C. O. Romero, J. S. Wong, J. Giner, R. Kumar, Monolithic Multiband MEMS RF Front-End Module for 5G Mobile, *Journal of Microelectromechanical Systems*, 30 (2021), 72–80, doi: 10.1109/JMEMS.2020.3036379
- <sup>8</sup> Rashad H. Mahmud, Halgurd N. Awl, Yadgar I. Abdulkarim, Muharrem Karaaslan, Michael J. Lancaster, Filtering two-element waveguide antenna array based on solely resonators, *AEU – International Journal of Electronics and Communications*, 121 (2020), 153232, doi:10.1016/j.aeue.2020.153232
- <sup>9</sup> S. Palanisamy, B. Thangaraju, O. I. Khalaf, Y. Alotaibi, S. Alghamdi, F. Alassery, A Novel Approach of Design and Analysis of a Hexagonal Fractal Antenna Array (HFAA) for Next-Generation Wireless Communication, *Energies*, 14 (2021), 6204, doi:10.3390/en14196204
- <sup>10</sup> Y. C. Li, H. Wong, Q. Xue, Dual-Mode Dual-Band Bandpass Filter Based on a Stub-Loaded Patch Resonator, *IEEE Microwave and Wireless Components Letters*, 21 (2021), 525–527, doi:10.1109/LMWC.2011.2164394
- <sup>11</sup> Z. Hou, C. Liu, B. Zhang, R. Song, Z. Wu, J. Zhang, D. He, Dual-/Tri-Wideband Bandpass Filter with High Selectivity and Adjustable Passband for 5G Mid-Band Mobile Communications, *Electronics*, 9 (2020), 205, doi:10.3390/electronics9020205
- <sup>12</sup> Dong-Sheng La, Xin Guan, Hong-Cheng Li, Yu-Ying Li, Jing-Wei Guo, Design of Broadband Band-Pass Filter with Cross-Coupled Line Structure, *International Journal of Antennas and Propagation*, 2020 (2020) 5, doi:10.1155/2020/5257325
- <sup>13</sup> Y. Wang, X.-Y. Zhang, F.-X. Liu, J.-C. Lee, A Compact Bandpass Wilkinson Power Divider with Ultra-Wide Band Harmonic Suppression, *IEEE Microwave and Wireless Components Letters*, 27 (2017), 888–890, doi: 10.1109/LMWC.2017.2745484
- <sup>14</sup> X. Zheng, Y. Pan, T. Jiang, UWB Bandpass Filter with Dual Notched Bands Using T-Shaped Resonator and L-Shaped Defected Microstrip Structure, *Micromachines*, 9 (2018) 280, doi:10.3390/mi9060280
- <sup>15</sup> N. A. Al-Shalaby, S. M. Gaber, Design of Defected Ground Structure Band Stop/Band Pass Filters Using Dielectric Resonator, *Wireless Pers. Commun.*, 109 (2019), 2427–2437, doi:10.1007/s11277-019-06690-7
- <sup>16</sup> S. Tantivivat, S. Z. Ibrahim, M. S. Razalli, Design of quad-channel diplexer and tri-band bandpass filter based on multiple-mode stub-loaded resonators, *Radioengineering*, 27 (2019), 129–135, doi: 10.13164/re.2019.0129
- <sup>17</sup> B. Ren, Z. Ma, H. Liu, X. Guan, P. Wen, X. Wang, O. Masataka, Miniature dual-band bandpass filter using modified quarter-wave-length SIRs with controllable passbands, *Electron. Lett.*, 55 (2018), 38–40, doi:10.1049/el.2018.6702
- <sup>18</sup> H. Y. D. Yang, J. Wang, Surface waves of printed antennas on planar artificial periodic dielectric structures, *IEEE Transactions on Antennas and Propagation*, 49 (2021), 444–450, doi:10.1109/8.918619
- <sup>19</sup> Jinchun Wang et al., Transparent graphene microstrip filters for wireless communications, *J. Phys. D: Appl. Phys.*, 50 (2017) 34, doi: 10.1088/1361-6463/aa7c99
- <sup>20</sup> Z. Hou, C. Liu, B. Zhang, R. Song, Z. Wu, J. Zhang, D. He, Dual-/Tri-Wideband Bandpass Filter with High Selectivity and Adjustable Passband for 5G Mid-Band Mobile Communications, *Electronics*, 9 (2020) 20, doi:10.3390/electronics9020205